J. Fluid Mech. (1995), *vol.* , *pp.*

Convection in ^{3}He-superfluid-^{4}He mixtures. Part I. A Boussinesq analogue

By GUY METCALFE[1] AND R.P. BEHRINGER[2]

[1]Division of Building, Construction and Engineering, CSIRO, Highett 3190, Australia

[2]Duke Univ. Dept. of Physics and Center for Nonlinear and Complex Systems, Durham NC 27708, USA

(Received September 26, 1994; revised July 5, 1995)

Appendix A. Fluid parameters for an $X = 0.0122$ superfluid mixture

To be able to calculate the Prandtl number and Rayleigh number for fluids undergoing superfluid mixture convection, we require several thermodynamic and hydrodynamic quantities measured from T_λ to about 0.4 K. Here we collect in one place and tabulate the needed data (Metcalfe 1991).

A.1. *Needed parameters*

The Rayleigh and Prandtl numbers are defined for superfluid mixtures as

$$Ra = \frac{|\alpha_{p,\mu_4}|\, g d^3 \Delta T}{\nu \chi_{eff}} \tag{A 1}$$

$$Pr = \frac{\nu_n}{\chi_{eff}} = \frac{\nu_n}{\kappa_{eff}} (\rho C_{p,\mu_4}). \tag{A 2}$$

We measure ΔT and d directly, but in order to construct these dimensionless numbers and the vertical thermal diffusion time τ_v, we need to know the remaining thermo-hydrodynamic quantities. C_{p,μ_4} and α_{p,μ_4} are not the standard specific heat and expansion coefficient and are not directly measured—they are both at constant ^{4}He chemical potential—but can be easily related to measured quantities. In this appendix we first calculate these relations and then tabulate all data needed to construct Ra and Pr for the temperature range 0.4–2.15 K.

Most of the notation in this appendix has been defined in §1. Graphs appear in text near where the data is discussed, but data tables are grouped at the end of this appendix. Unless otherwise noted, parameters are for an $X = 0.0122$ superfluid mixture.

A.2. C_{p,μ_4} *and* α_{p,μ_4}

The specific heat/mass at constant ^{4}He chemical potential and pressure is defined (Fetter 1982) as

$$C_{p,\mu_4} = Tc \left[\frac{\partial(s/c)}{\partial T}\right]_{p,\mu_4} \tag{A 3}$$

and requires a thermodynamic change of variables to eliminate μ_4. Lowercase s is the entropy per mass, and s/c is the entropy per ^{3}He mass. Expanding the derivative, we find that

$$C_{p,\mu_4} = T(\partial s/\partial T)_{p,\mu_4} - (Ts/c)(\partial c/\partial T)_{p,\mu_4}. \tag{A 4}$$

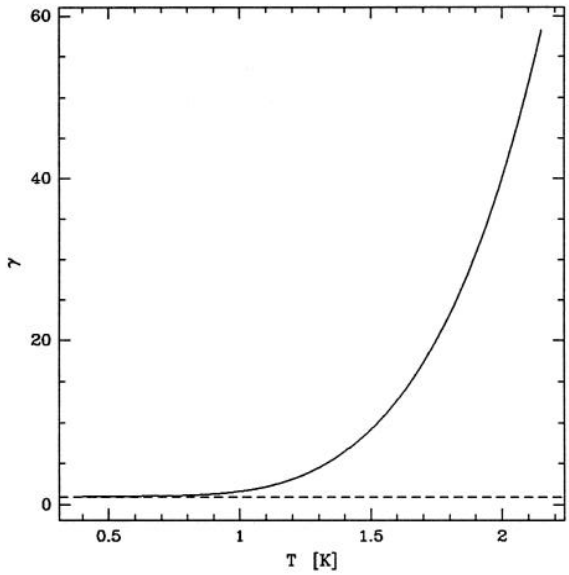

FIGURE 16. The coupling parameter γ.

The second term can be written as a ratio of derivatives of μ_4 with respect to T and c. Fetter (1982) parameterizes this ratio via the constant γ. γ is the constant of proportionality between the temperature and concentration fields under the condition $\nabla\mu_4 = \rho g$, i.e. the condition of the ^{4}He chemical potential not deviating from its equilibrium profile. For a dilute mixture

$$\gamma \equiv \frac{T}{c}\frac{(\partial\mu_4/\partial T)_{c,p}}{(\partial\mu_4/\partial c)_{T,p}} = 1 + \frac{s_4}{k_B c}, \tag{A 5}$$

where s_4 is the entropy/gram of pure ^{4}He and k_B is Boltzmann's constant. Figure 16 shows γ with s_4 taken from the tables of Brooks and Donnelly (BD) (1977). The dashed line is $\gamma = 1$. Note that above about 1 K, γ rises rapidly above 1 as s_4 increases.

The first term of Equation A 4 can be transformed by, for instance, Jacobians (Callen 1960) from the variables (T, μ_4) to (T, c). With that transformation

$$C_{p,\mu_4} = C_{p,c} + \gamma\left[s - c\,(\partial s/\partial c)_{T,p}\right], \tag{A 6}$$

but the quantity measured and tabulated is S, the entropy per mole. The entropy per mole and per mass are related by $S = sM$, where $M = Xm_3 + (1-X)m_4$ is the mass per mole. Finally we find that

$$m_4 C_{p,\mu_4} = C_{p,X} + \gamma\left[\left(\frac{M}{m_4}\right)S - X\,(\partial S/\partial X)_{T,p}\right]. \tag{A 7}$$

Equation A 7 is valid for a dilute solution. C_{p,μ_4} remains the specific heat per mass, but $C_{p,X}$ is the specific heat per mole.

In similar fashion the expansion coefficient is transformed to

$$\alpha_{p,\mu_4} = \alpha_{p,X} - \frac{\gamma c}{T}\beta_c \tag{A 8}$$

where $\beta_c = -\rho^{-1}(\partial\rho/\partial c)_{p,T}$.

A.3. *Tabulations*

We chose to represent all data with cubic B-splines (deBoor 1978) that provide a best fit to the data in a least-squares sense. As has been previously pointed out by Donnelly (Barenghi et al. 1981; Donnelly et al. 1981), splines are well suited to representing thermodynamic data in the presence of phase transitions. This is because splines, unlike other smooth functions (polynomials for example), allow the analyst complete control of the *point-wise* smoothness of the spline. This is accomplished through the placement of coincident knots. For example, with a cubic spline if we place 3 knots at T_λ, then the function's first derivative will jump at T_λ but the the function will retain continuity through the 2nd derivative at all other points. Being interested here only in the superfluid phase (for superfluid mixture convection), we do not take full advantage of this property.

A `Fortran` program to reproduce the tabulated data for any temperature in the range $0.4 \leq T \leq 2.15$ is available from the authors on request. The workhorses in our program are the routines that calculate the splines: `SPFIT`, `SCOMP`, and `SEVAL` from the Naval Surface Warfare Center Mathematical Subroutine Library (Morris 1990). Knot placement follows the simple scheme of de Boor (1978, p. 219), and no attempt was made to find a minimum or optimal number of knots. In this appendix the solid curves in graphs are spline fits and points are data. Generally, the absolute deviation of the spline from the data is a few tenths of a percent with maximum deviations of at most a few percent. In every case the spline deviation is well within the data's accuracy.

A.3.1. *density*

For use with viscosity measurements, Howald (1991) has fit Kierstead's (1976) data for the density of helium mixtures in the T–X plane. The density of the fluid is measured capacitatively to 0.001% through changes in the dielectric constant (Kierstead 1976). The density of the mixture is shown as the top line in Figure 17 and on an expanded scale in the inset figure. Howald's fit covers $0.95 < T < 4$ K. Below this range we use density data based on the molar volume v_m measurements of Kerr & Taylor (1964) of pure ^{4}He. Data on v_m from Ifft et al. [shown as Figure 10 of Ebner & Edwards (1971)] and Kakizaki & Satoh (1976) show that $X = 0.04$ mixtures differ in v_m by only 1% from pure ^{4}He over the entire temperature range of interest here, and of course that difference decreases with X. However, the densities from Kerr & Taylor were multiplied by 0.996968 to exactly match Howald's fit of Kierstead's data at 0.95 K.

Since the term representing momentum diffusion in Pr is the "normal" kinematic viscosity, we also need the normal fluid density ρ_n. Sobolov et al. (Grigor'ev et al. 1967; Sobolov & Esel'son 1971) have measured ρ_n for a variety of concentrations, and Howald (1991) has fit the Sobolov data over the T-X plane. Below 0.95 K we took

$$\rho_n = n_3 m^* + \rho_{no}, \tag{A 9}$$

where ρ_{no} is the normal density of pure ^{4}He, n_3 is the number density of ^{3}He atoms, and m^* is the effective mass of a ^{3}He quasiparticle. Ebner and Edwards (1971) show that

$$\rho_n = \frac{N_A X \rho m_3}{m_4}(a + bT) + \rho_{no} \tag{A 10}$$

for a dilute solution, where $m^* = m_3(a + bT)$ and a and b are calculable in principle but, in fact are experimentally determined, and N_A is Avagadro's number. Brubaker's et al. measurements of m^* [shown as Figure 21 of Ebner & Edwards (1971)] give $a = 2.214$ and $b = 0.914$ to about 1.5%, but only below 0.6 K; we assume it is valid to extend the relation to higher temperatures. We multiplied Equation A 10 by 0.908 to make it match up smoothly at 0.95 K with Howald's fit of the Sobolov data. The BD tables supply ρ_{no}.

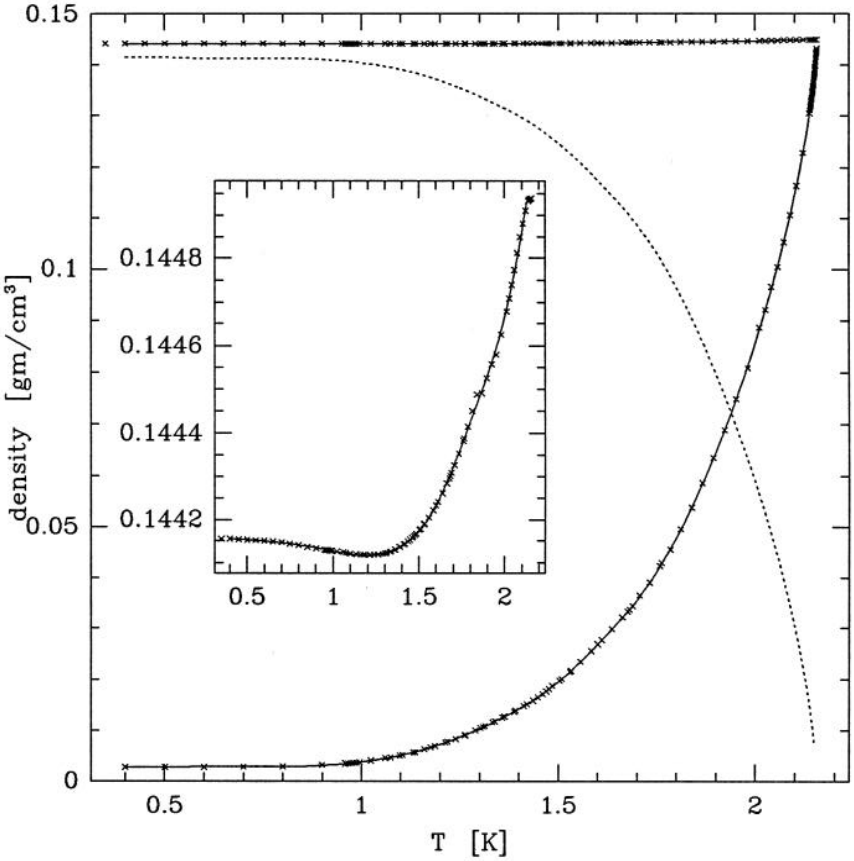

FIGURE 17. The top curve is the total fluid density ρ, which is also shown in the inset on an expanded density scale. The lower curve is the normal fluid density ρ_n. For comparison the dotted line shows the superfluid density $\rho_s = \rho - \rho_n$.

ρ_n is the lower curve in Figure 17. For comparison the dotted line in the figure shows the superfluid density $\rho_s = \rho - \rho_n$.

Figure 18 shows various expansion coefficients. $\alpha_{p,X}$ $(= -\rho^{-1}\,(\partial\rho/\partial T)_{p,X})$ is a derivative of the spline, so it is as accurate as the data for ρ. β_c $(= -\rho^{-1}\,(\partial\rho/\partial c)_{T,X})$ comes from writing the density (Ebner & Edwards 1971; Lucas & Tyler 1977) as

$$\rho = \frac{X m_3 + (1-X) m_4}{v_4(1+\alpha X)}, \tag{A 11}$$

and differentiating. v_4 is the molar volume of pure ^{4}He and α scales the increase in molar volume from adding ^{3}He atoms into solution. Ebner & Edwards (1971) give a table of α from 0–1 K based on data and theory. A fit to their values for zero concentration gives $\alpha = 0.284 - 0.032\,T$ to an accuracy of about 2%. We assume that it is valid to extend this relation for α above 1 K. With $\alpha_{p,X}$, β_c and γ in hand, we show α_{p,μ_4} at the top of Figure 18.

A.3.2. *specific heat*

Equation A 7 relates C_{p,μ_4} to the entropy, its derivatives in X and T, and the entropy of pure ^{4}He. To obtain $C_{p,X}$, we have interpolated between de Bruyn Ouboter et al.'s (1960) measurements of $C_{p,X}$ for $X = 0.0466$ and the tabulation by BD of C_p for pure

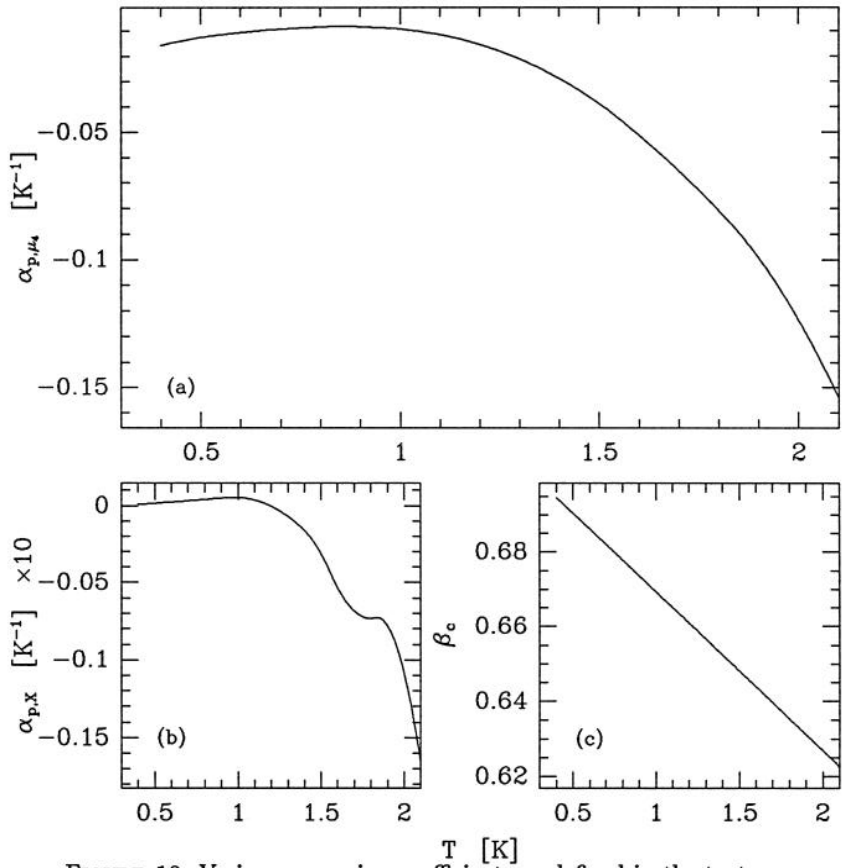

FIGURE 18. Various expansion coefficients as defined in the text.

^{4}He. Since the Ouboter data becomes unsuitable for interpolation above 2.105 K (T_λ for $X = 0.0466$), we extend the Ouboter curve to 2.15 K by extrapolating a straight line using the slope at 2.082 K. The data of Ouboter and BD and the interpolated $C_{p,X}$ are shown in Figure 19. Integration of $C_{p,X}$ then produces the entropy S. The integration constant was chosen based on the data in Zhong's dissertation (1989, pp. 153–155) to be $S = 4.75$ J/mole K at $T = 2.0$ K. The derivative $(\partial S/\partial X)_{p,T}$ was differenced from S and S_4.

Figure 20 shows C_{p,μ_4}. The inset figure shows the ratio of $C_{p,X}$ to C_{p,μ_4}. This ratio gives some feel for how much of the thermal "mass" is due to classical thermal modes. Note that below 1 K, C_{p,μ_4} is almost entirely due to $C_{p,X}$, but as $T \to T_\lambda$, small differences in X cause large changes in the entropy for dilute mixtures: most of C_{p,μ_4} is then from $(\partial S/\partial X)_{p,T}$.

A.3.3. *viscosity*

Using an oscillating disk viscometer (Howald 1991; Agosta et al. 1987), Howald & Meyer were kind enough to measure the shear viscosity η of an extra portion of our sample mixture with an absolute accuracy of 2%. (The viscosity and density are for an $X = 0.0119$ mixture because some of the ^{3}He adsorbs onto the activated charcoal in liquid nitrogen traps when the mixture is condensed into the viscometer. For our purposes, we ignore this small concentration change.) From η, ρ and ρ_n, we are able to tabulate the

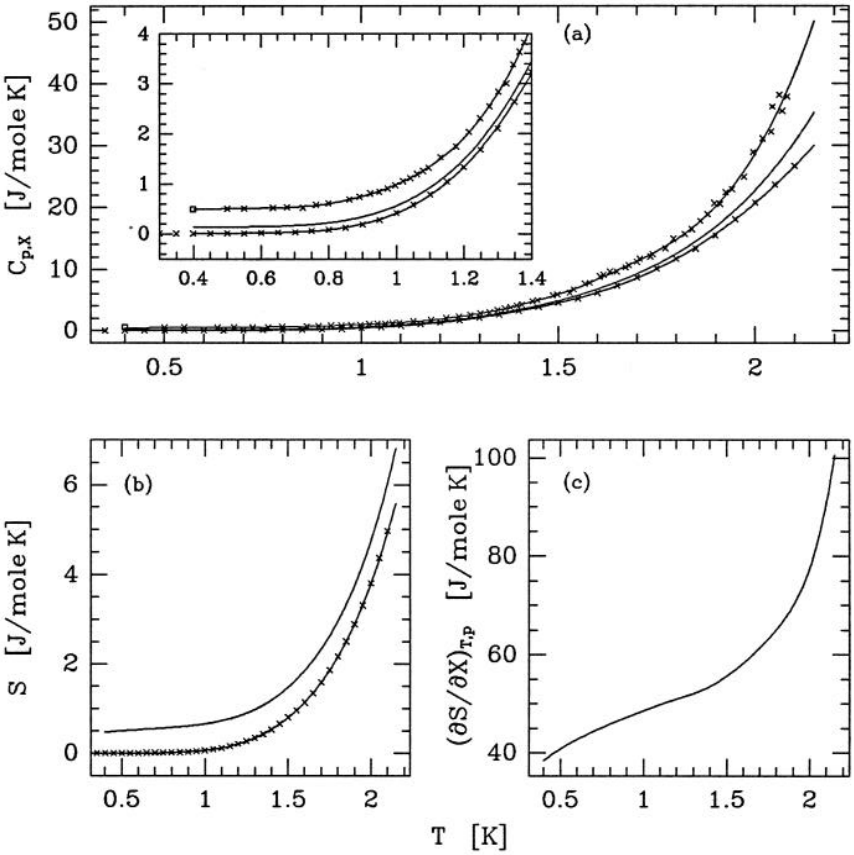

FIGURE 19. Entropy and its derivatives with respect to T and X. In part (a) the top curve is $X = 0.0466$. The open square is a calculated point from Radebaugh (1967). The bottom curve is for pure ^{4}He. The middle curve is the interpolation for $X = 0.0122$. The inset shows $C_{p,X}$ on an expanded scale at lower temperatures. In part (b) the lower curve shows the entropy for pure ^{4}He. The derivative in part (c) is differenced from the two curves in part (b).

regular and "normal" kinematic viscosities for use in Ra and Pr. The upper curve in Figure 21 shows ν_n while the lower line shows ν. They are related by $\nu = (\rho_n/\rho)\nu_n$. The three lowest temperature points are from Kuenhold et al. (1972), who used flow through fine capillaries to measure η for an $X = 0.013$ mixture. The Kuenhold et al. data have been multiplied by 1.659 in order to make them match Howald's. This factor was chosen by extending a line with the slope of Howald's data at 1 K to 0.6 K and forcing Kuenhold et al.'s data to match this line at 0.6 K. This is an unsatisfactory procedure, but the unchanged data is shown in Figure 21 as open circles, and it is hard to believe that η really changes so sharply as to make these data sets match. We chose to believe the data of Howald & Meyer. On the other hand, the lowest temperature for which data is needed is defined by the minimum in $Pr(T)$, which is about 0.6 K (figure 2). We may point out that, if we do take ν_n to be lower, more in accord with the Kuenhold et al. data, then the minimum Prandtl number will be *lowered* by this factor of 1.6, broadening the available Prandtl number range of superfluid mixtures even further. We also note that in the experiments reported in these papers 0.8 K was the lowest temperature used.

A.3.4. *conductivity*

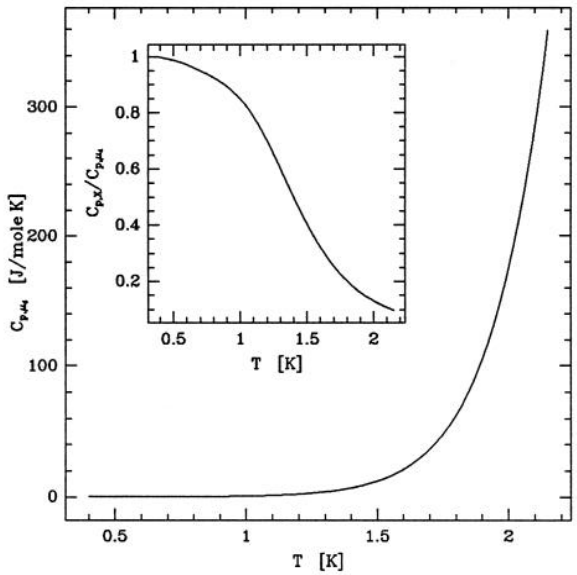

FIGURE 20. Specific heat at constant ^{4}He chemical potential. The inset shows the ratio $C_{p,X}/C_{p,\mu_4}$.

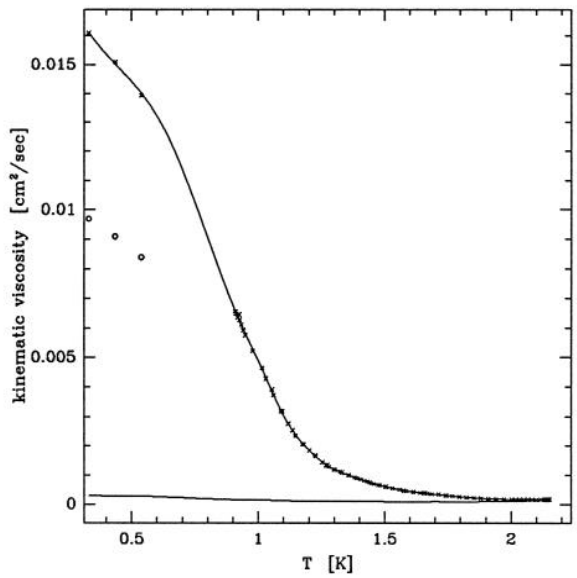

FIGURE 21. The top curve is "normal" kinematic viscosity ν_n. The bottom line is standard kinematic viscosity $\nu = (\rho_n/\rho)\nu_n$. The open circles are unnormalized data from (Kuenhold et al. 1972), as discussed in the text.

Shown in Figure 22 are conductivity data for several dilute superfluid mixtures. The solid circles and triangles are from Murphy & Meyer (private communication) of Duke University and are part of an ongoing program to measure the conductivity of ^{3}He-^{4}He mixtures (Tuttle 1991). These data have about 1% accuracy. The solid squares are from the Los Alamos group (Hauke 1987) and have 3% accuracy. The open squares are the data of Ptukha (1961) and are accurate to about 10%. Our own data for several temperatures and many cell heights are shown as crosses in Figure 22. We have already

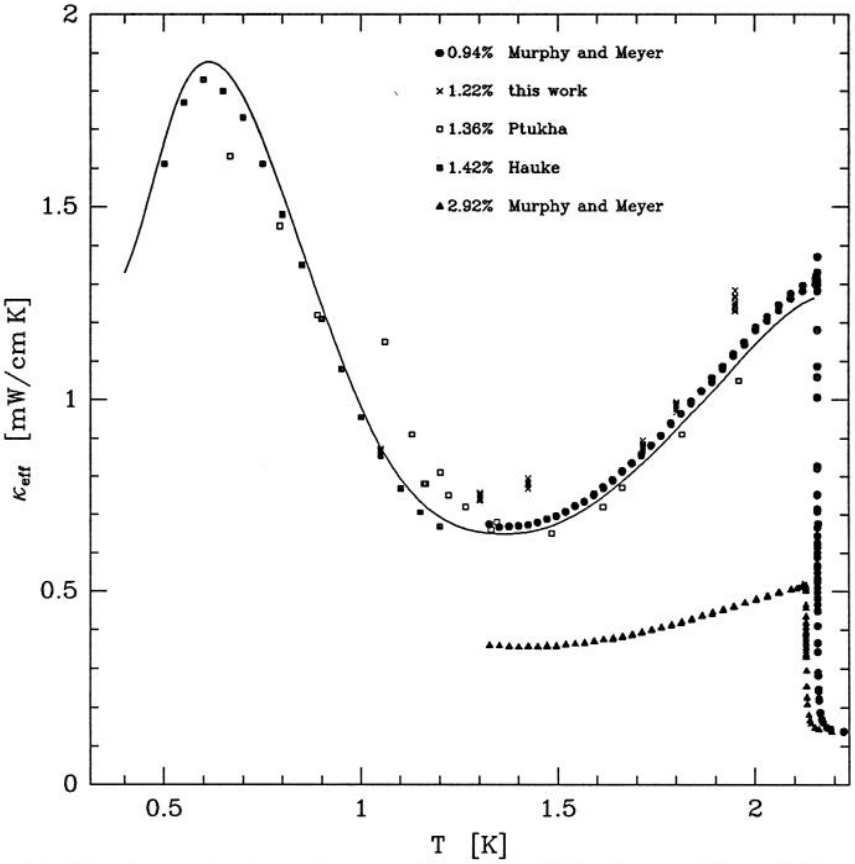

FIGURE 22. Effective conductivity of several dilute superfluid mixtures. The solid line is an estimate for $X = 1.22\%$ interpolating between the 0.94% and 1.46% mixtures.

discussed in §2.5 the corrections applied to the measured conductance in order to obtain κ_{eff}. At a given temperature we determine κ_{eff} for any number of cell heights. Our statistical error for C_t at a given height is less than 1%. It is evident that the error associated with differing heights is larger but still less than 5%. However, the absolute accuracy of our determinations of κ_{eff} must be in error by about 10%, judging from the more accurate measurements of Murphy & Meyer, although, the shape of the curve seems to be correct. We believe this inaccuracy reflects our imprecise knowledge of the heat flux carried by our cell walls. The maximum in κ_{eff} near 0.7 K accounts for the Pr minimum seen in Figure 2.

For the purpose of calculation, we decreased the data of Murphy and Meyer by 3% and increased that of Los Alamos by a like amount to piece together the solid line in Figure 22. The line gives κ_{eff} from 0.4 to 2.15 K to about 3% accuracy.

A.3.5. *derived parameters*

Our main aim in this appendix has been to calculate Ra, Pr and τ_v. Figure 23 shows the combination $\nu\chi_{eff}/|\alpha_{p,\mu_4}|g$, which scales $d^3\Delta T$ in Ra. Figure 24 shows χ_{eff} from which we can construct the time scale τ_v for any given cell height. The inset to Figure 24 shows τ_v assuming a 1 cm tall cell. Figure 2 shows Pr for the $X = 0.0122$ mixture along with Pr for pure ^{4}He and two other dilute mixtures used by the Los Alamos group. For

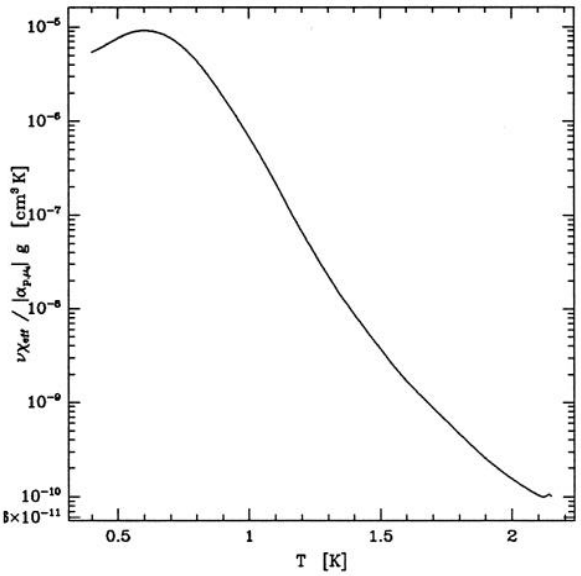

FIGURE 23. Semilog plot of the parameter group scaling $d^3\Delta T$ in the Rayleigh number as a function of temperature. This is also $T\Lambda_o^3$ (Metcalfe & Behringer 1991; Metcalfe 1991).

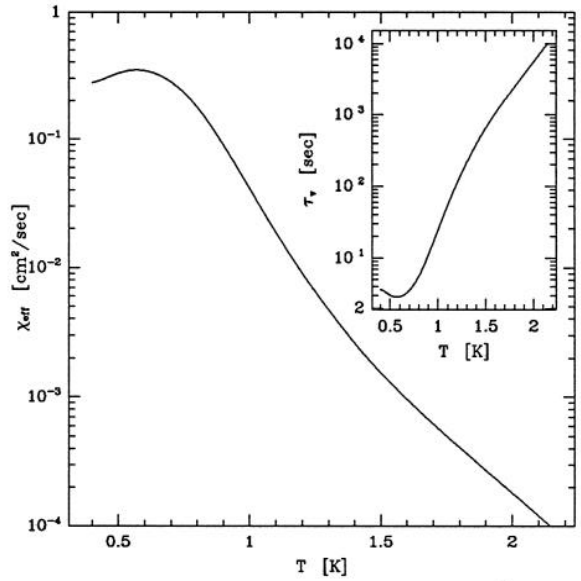

FIGURE 24. The effective thermal diffusivity. The inset shows χ_{eff}^{-1} or the vertical thermal diffusion time τ_v calculated assuming a 1 cm tall cell.

---

the $X = 0.0122$ mixture, Figure 2 shows the complete, and astoundingly large, range $0.04 < Pr < 1.5$.

A.4. *Tables*

Tables 2–4 are evaluations at 0.1 degree intervals from 0.4 to 2.1 K of the splines representing the data discussed above.

T	S	$C_{p,X}$	$(\partial S/\partial X)_{T,X}$	C_{p,μ_4}
K	J/mole K	J/mole K	J/mole K	J/mole K
0.4	4.188e-01	1.336e-01	3.419e+01	1.340e-01
0.5	4.494e-01	1.394e-01	3.657e+01	1.412e-01
0.6	4.753e-01	1.465e-01	3.850e+01	1.509e-01
0.7	4.991e-01	1.678e-01	4.012e+01	1.768e-01
0.8	5.246e-01	2.221e-01	4.162e+01	2.400e-01
0.9	5.570e-01	3.425e-01	4.300e+01	3.835e-01
1.0	6.036e-01	5.629e-01	4.434e+01	6.627e-01
1.1	6.728e-01	9.258e-01	4.560e+01	1.177e+00
1.2	7.752e-01	1.489e+00	4.667e+01	2.121e+00
1.3	9.230e-01	2.309e+00	4.763e+01	3.836e+00
1.4	1.131e+00	3.451e+00	4.883e+01	6.899e+00
1.5	1.416e+00	4.926e+00	5.081e+01	1.218e+01
1.6	1.797e+00	6.841e+00	5.387e+01	2.122e+01
1.7	2.296e+00	9.326e+00	5.808e+01	3.662e+01
1.8	2.937e+00	1.253e+01	6.353e+01	6.237e+01
1.9	3.745e+00	1.686e+01	7.005e+01	1.050e+02
2.0	4.750e+00	2.272e+01	7.756e+01	1.742e+02
2.1	5.982e+00	3.051e+01	8.613e+01	2.836e+02

TABLE 2. Thermodynamic data for an $X = 0.0122$ superfluid mixture.

T	ρ	ρ_n	$\alpha_{p,X}$	β_c	α_{p,μ_4}
K	gm/cm^3	gm/cm^3	K^{-1}	—	K^{-1}
0.4	1.442e-01	2.723e-03	8.812e-05	6.948e-01	-1.581e-02
0.5	1.442e-01	2.747e-03	1.631e-04	6.905e-01	-1.267e-02
0.6	1.442e-01	2.854e-03	2.409e-04	6.863e-01	-1.065e-02
0.7	1.441e-01	2.849e-03	3.215e-04	6.820e-01	-9.316e-03
0.8	1.441e-01	2.863e-03	4.048e-04	6.778e-01	-8.537e-03
0.9	1.441e-01	3.110e-03	4.909e-04	6.736e-01	-8.483e-03
1.0	1.441e-01	3.795e-03	5.392e-04	6.693e-01	-9.352e-03
1.1	1.441e-01	5.054e-03	3.690e-04	6.651e-01	-1.157e-02
1.2	1.441e-01	7.203e-03	-4.107e-05	6.608e-01	-1.545e-02
1.3	1.441e-01	1.032e-02	-6.984e-04	6.566e-01	-2.117e-02
1.4	1.441e-01	1.416e-02	-1.616e-03	6.524e-01	-2.881e-02
1.5	1.442e-01	1.949e-02	-3.157e-03	6.481e-01	-3.876e-02
1.6	1.442e-01	2.679e-02	-5.355e-03	6.439e-01	-5.128e-02
1.7	1.443e-01	3.558e-02	-6.849e-03	6.396e-01	-6.532e-02
1.8	1.444e-01	4.784e-02	-7.334e-03	6.354e-01	-8.088e-02
1.9	1.445e-01	6.466e-02	-7.822e-03	6.311e-01	-9.935e-02
2.0	1.447e-01	8.571e-02	-1.088e-02	6.269e-01	-1.237e-01
2.1	1.449e-01	1.144e-01	-1.664e-02	6.227e-01	-1.541e-01

TABLE 3. More thermodynamic data for an $X = 0.0122$ superfluid mixture.

T K	ν_n cm^2/sec	κ_{eff} mW/cm K	χ_{eff} cm^2/sec	Pr —	$\nu\chi_{eff}/\lvert\alpha_{p,\mu_4}\rvert g$ cm^3 K
0.4	1.611E-02	1.330e+00	2.754e-01	5.851e-02	5.405e-06
0.5	1.503E-02	1.668e+00	3.276e-01	4.586e-02	7.549e-06
0.6	1.401E-02	1.874e+00	3.446e-01	4.065e-02	9.150e-06
0.7	1.253E-02	1.786e+00	2.804e-01	4.468e-02	7.599e-06
0.8	1.035E-02	1.534e+00	1.774e-01	5.833e-02	4.357e-06
0.9	7.908E-03	1.244e+00	9.005e-02	8.782e-02	1.847e-06
1.0	5.747E-03	9.810e-01	4.108e-02	1.399e-01	6.779e-07
1.1	3.805E-03	7.934e-01	1.871e-02	2.034e-01	2.200e-07
1.2	2.232E-03	6.929e-01	9.066e-03	2.462e-01	6.675e-08
1.3	1.388E-03	6.537e-01	4.730e-03	2.935e-01	2.265e-08
1.4	9.680E-04	6.500e-01	2.615e-03	3.702e-01	8.804e-09
1.5	6.811E-04	6.765e-01	1.542e-03	4.418e-01	3.734e-09
1.6	4.778E-04	7.351e-01	9.606e-04	4.974e-01	1.695e-09
1.7	3.689E-04	8.193e-01	6.201e-04	5.948e-01	8.802e-10
1.8	2.730E-04	9.213e-01	4.091e-04	6.673e-01	4.665e-10
1.9	2.055E-04	1.029e+00	2.711e-04	7.581e-01	2.558e-10
2.0	1.748E-04	1.142e+00	1.813e-04	9.643e-01	1.549e-10
2.1	1.650E-04	1.236e+00	1.203e-04	1.371e+00	1.037e-10

TABLE 4. Hydrodynamic data for an $X = 0.0122$ superfluid mixture.

REFERENCES

AGOSTA, C.C., WANG, S., COHEN, L.H. & MEYER, H. 1987 Transport properties of helium near the liquid-vapor critical point. iv. the shear viscosity of ^{3}He and ^{4}He. *J. Low Temp. Phys.* **67**, 237–289.

BARENGHI, C.F., LUCAS, P.G.J. & DONNELLY, R.J. 1981 Cubic spline fits to thermodynamic and transport parameters of liquid ^{4}He above the λ transition. *J. Low Temp. Phys.* **44**, 491–504.

BROOKS, J.S. & DONNELLY, R.J. 1977 The calculated thermodynamic properties of superfluid helium-4. *J. Phys. Chem. Ref. Data* **6**, 51–104.

CALLEN, H.B. 1960 Thermodynamics. John Wiley.

DE BOOR, C. 1978 A Practical Guide to Splines. Springer-Verlag.

DE BRUYN OUBOTER, R., TACONIS, K.W., LE PAIR C. & BEENAKKER, J.J.M 1960 Thermodynamic properties of liquid ^{3}He-^{4}He mixtures derived from specific heat measurments between 0.4 K and 2 K over the complete concentration range. *Physica* **26**, 853–888.

DONNELLY, R.J., DONNELLY, J.A. & HILLS, R.N. 1981 Specific heat and dispersion curve for helium II. *J. Low Temp. Phys.* **44**, 471–489.

EBNER, C. & EDWARDS, D.O. 1971 The low temperature thermodynamic properties of superfluid solutions of ^{3}He in ^{4}He. *Phys. Reports* **2C**, 77–154.

FETTER, A. L. 1982 Onset of convection in dilute superfluid ^{3}He–^{4}He mixtures: Unbounded slab. *Phys. Rev. B* **26**, 1164–1173; Onset of convection in dilute superfluid ^{3}He–^{4}He mixtures: Closed cylindrical container. *Phys. Rev. B* **26**, 1174–1181.

GRIGOR'EV, V.N., ESEL'SON, B.N., MAL'KHANOV, V.P & SOBOLOV, V.I. 1967 Density of the normal component in concentrated helium isotope solutions. *Soviet Physics JETP* **24**, 707–710.

HAUCKE, H. 1987 Time-dependent convection in a ^{3}He-superfluid-^{4}He solution. PhD thesis, University of California San Diego.

HOWALD, C.D. 1991 Shear Viscosity Measurements in Liquid ^{3}He–^{4}He Mixtures near the Tricritical Point. PhD thesis Duke University.

KAKIZAKI, A. & SATOH, T. 1976 Thermodynamic properties of ^{3}He–^{4}He mixtures near T_λ. *J.*

Low Temp. Phys. **24**, 67–84.

KERR, E.C. & TAYLOR, R.D. 1964 The molar volume and expansion coefficient of liquid ^{4}He. *Ann. Phys.* **26**, 292–306.

KIERSTEAD, H.A. 1976 Dielectric constant, molar volume, and phase diagram of saturated liquid ^{3}He–^{4}He mixtures. *J. Low Temp. Phys.* **24**, 497–512.

KUENHOLD, K.A., CRUM, D.B. & SARWINSKI, R.E. 1972 The viscosity of dilute solutions of ^{3}He in ^{4}He at low temperatures. *Physics Letters* **41A**, 13–14.

LUCAS, P. & TYLER, A. 1977 Thermal diffusion ratio of a ^{3}He/^{4}He mixture near its λ transition: the onset of heat flush. *J. Low Temp. Phys.* **27**, 281–303.

METCALFE, GUY 1991 Using Superfluid Mixtures to Probe Convective Instabilities. PhD thesis, Duke University.

METCALFE, GUY & BEHRINGER, R.P. 1991 Critical Rayleigh numbers for cryogenic experiments. *J. Low Temp. Phys.* **78**, 231–246.

MORRIS, A.H. 1990 NSWC Library of Mathematics Subroutines. NSWC report TR 90–21, Dahlgren VA 22448.

PTUKHA, T.P. 1961 Thermal conductivity and diffusion in weak ^{3}He-^{4}He solutions in the temperature range from the λ point to 0.6 K. *Soviet Physics JETP* **13**, 1112–1119.

RADEBAUGH, R. 1967 Thermodynamic properties of ^{3}He-^{4}He solutions with applications to the ^{3}He-^{4}He dilution refrigeratior. National Bureau of Standards Technical Note 362.

SOBOLOV, V.I. & ESEL'SON, B.N. 1971 Normal component density of ^{3}He-^{4}He solutions at temperatures down to 0.4 K. *Soviet Physics JETP* **33**, 132–137.

TUTTLE, J.G. 1991 Thermal transport properties in dilute ^{3}He-^{4}He mixtures near the superfluid transition. PhD thesis, Duke University.

ZHONG, F. 1989 The thermal transport properties of dilute ^{3}He-^{4}He mixtures near the superfluid transition temperatures. PhD thesis, Duke University.

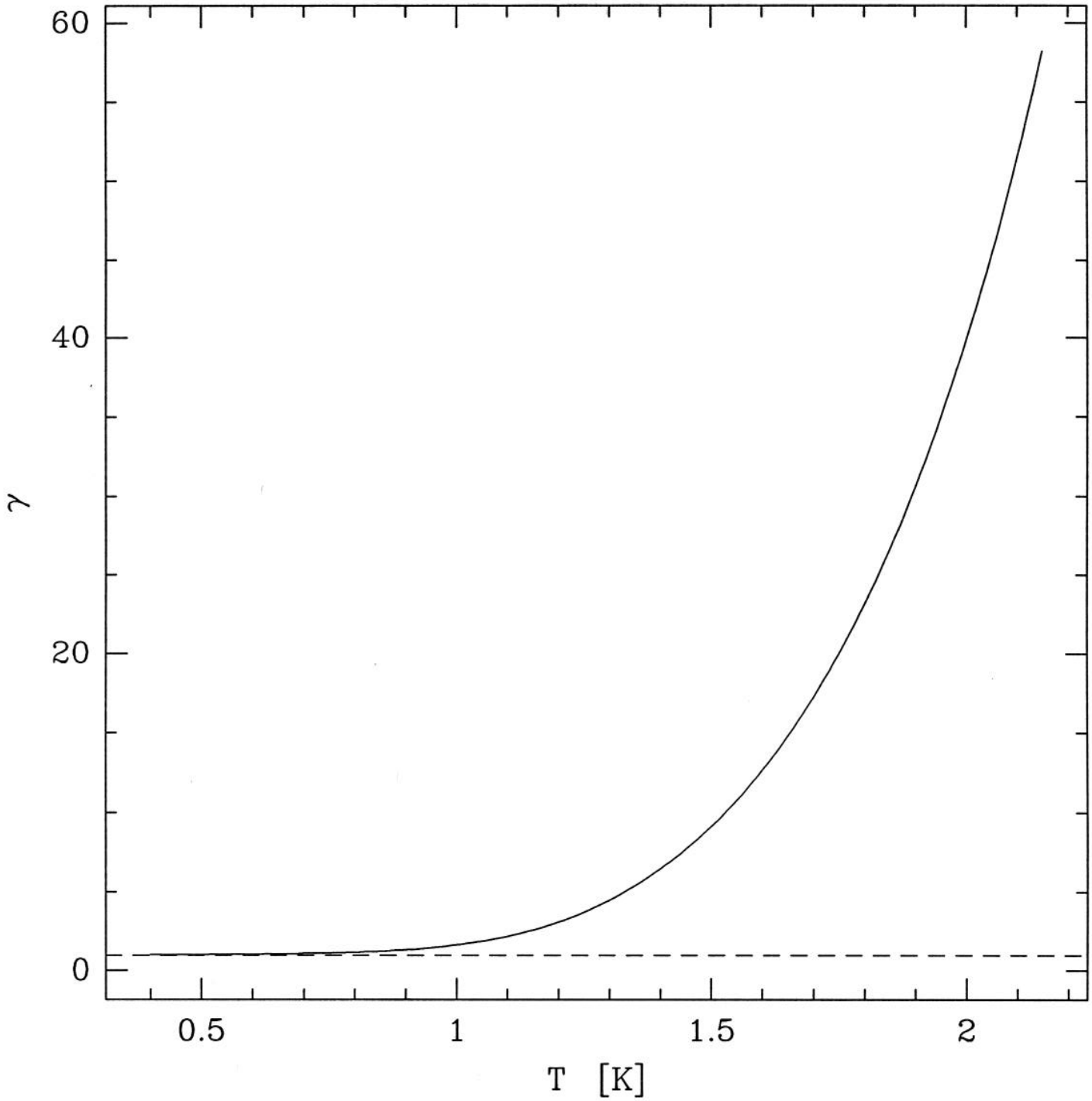
60
40
20
0
γ
0.5
1
1.5
2
T [K]

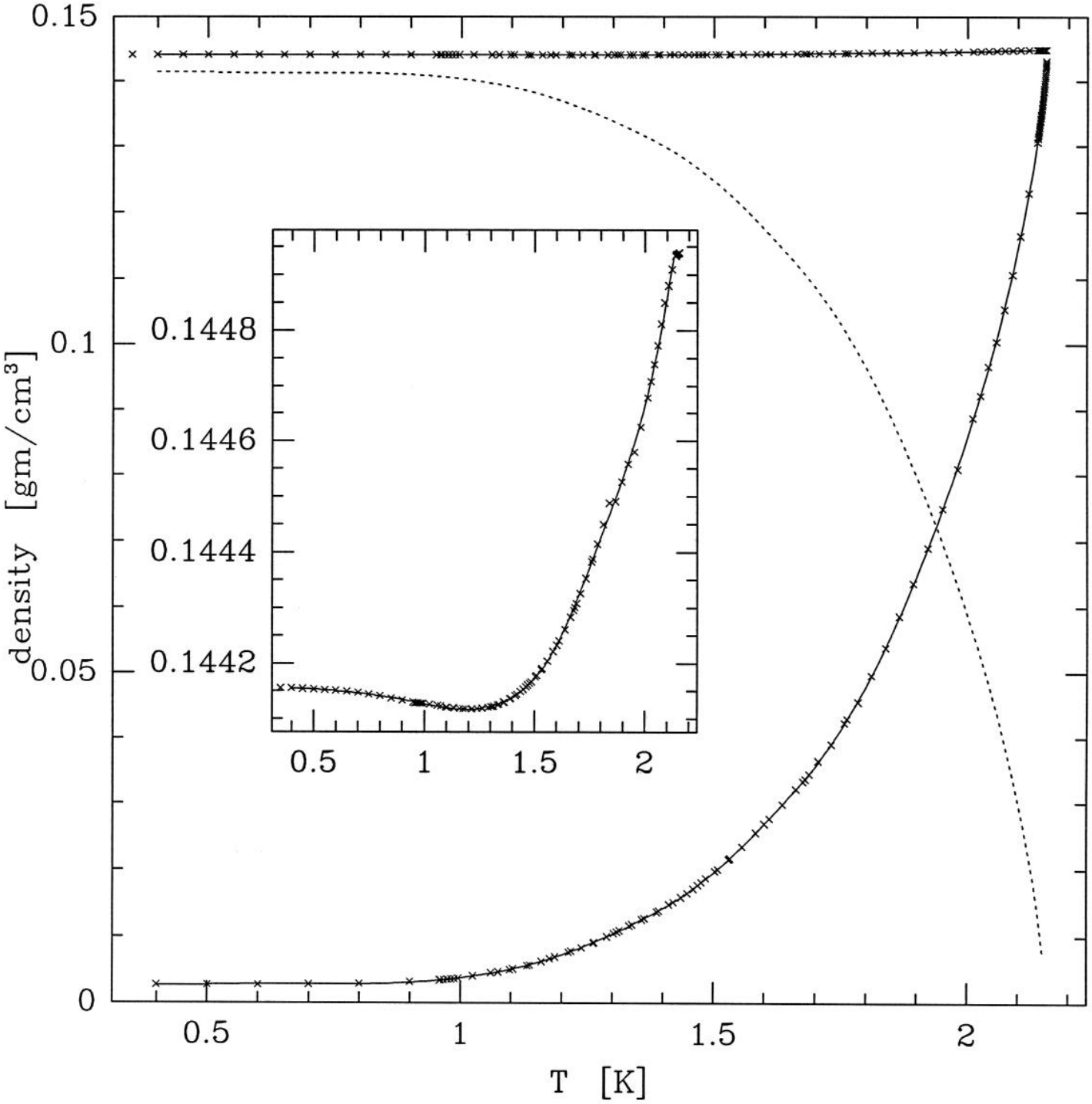
0.15
0.1
0.05
0
density [gm/cm^3]
0.5
1
1.5
2
T [K]
0.1448
0.1446
0.1444
0.1442
0.5
1
1.5
2

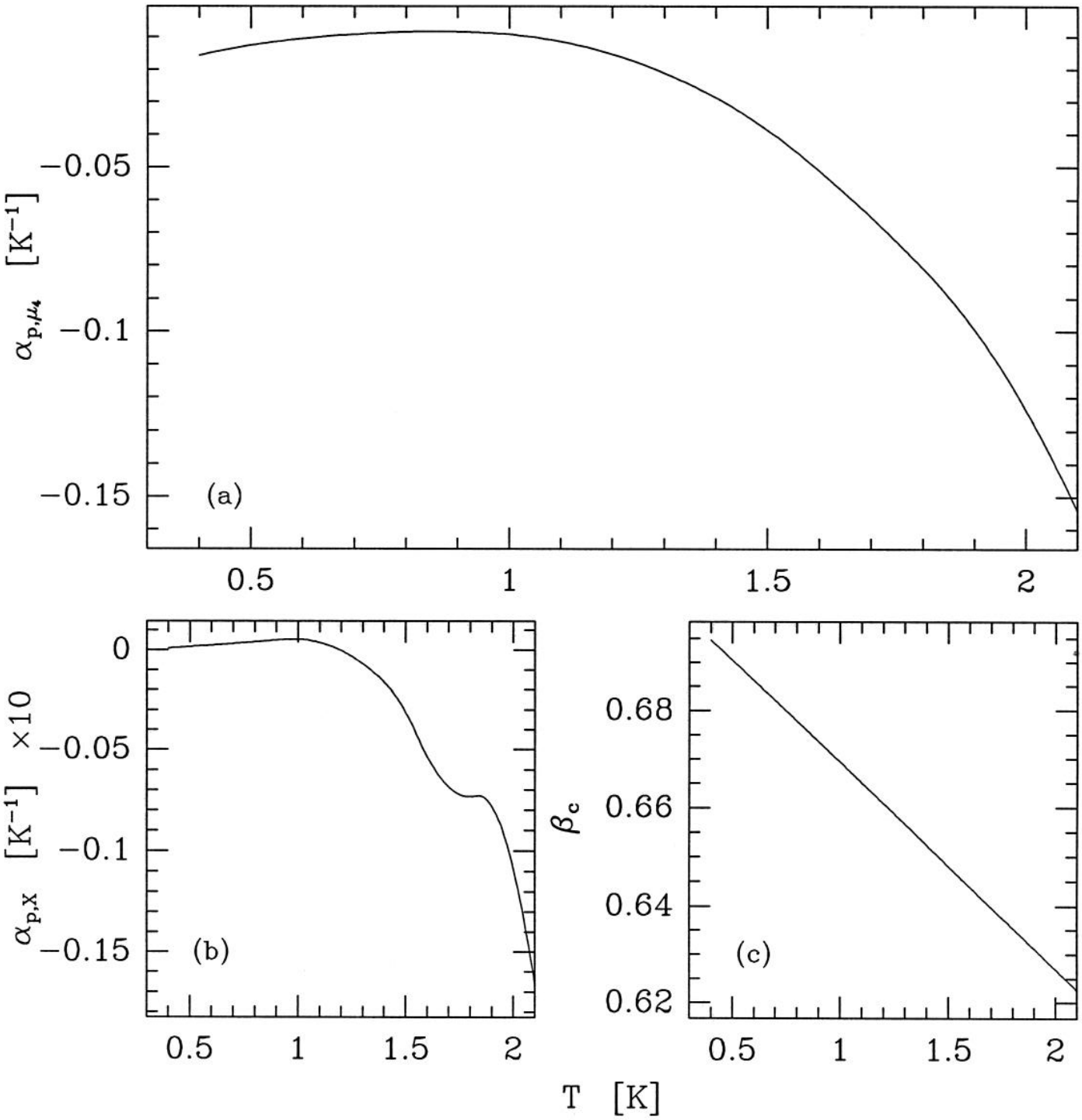
−0.05
−0.1
−0.15
α_{p,μ_4} [K^{-1}]
(a)
0.5
1
1.5
2
0
−0.05
−0.1
−0.15
$\alpha_{p,x}$ [K^{-1}] ×10
(b)
0.5
1
1.5
2
0.68
0.66
0.64
0.62
β_c
(c)
0.5
1
1.5
2
T [K]

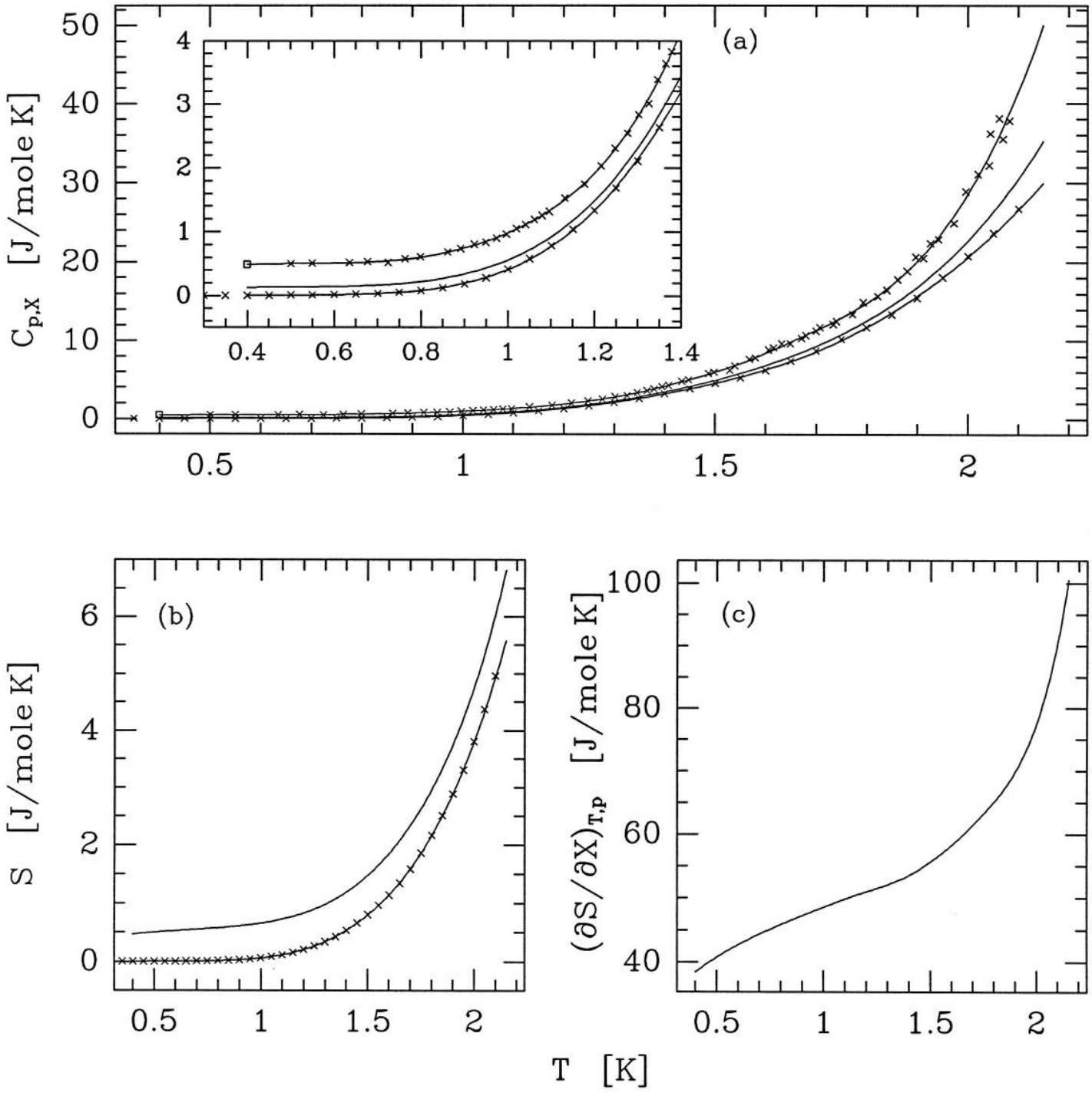
(a)
$C_{p,X}$ [J/mole K]
50
40
30
20
10
0
0.5
1
1.5
2
4
3
2
1
0
0.4
0.6
0.8
1
1.2
1.4
(b)
S [J/mole K]
6
4
2
0
0.5
1
1.5
2
(c)
$(\partial S/\partial X)_{T,p}$ [J/mole K]
100
80
60
40
0.5
1
1.5
2
T [K]

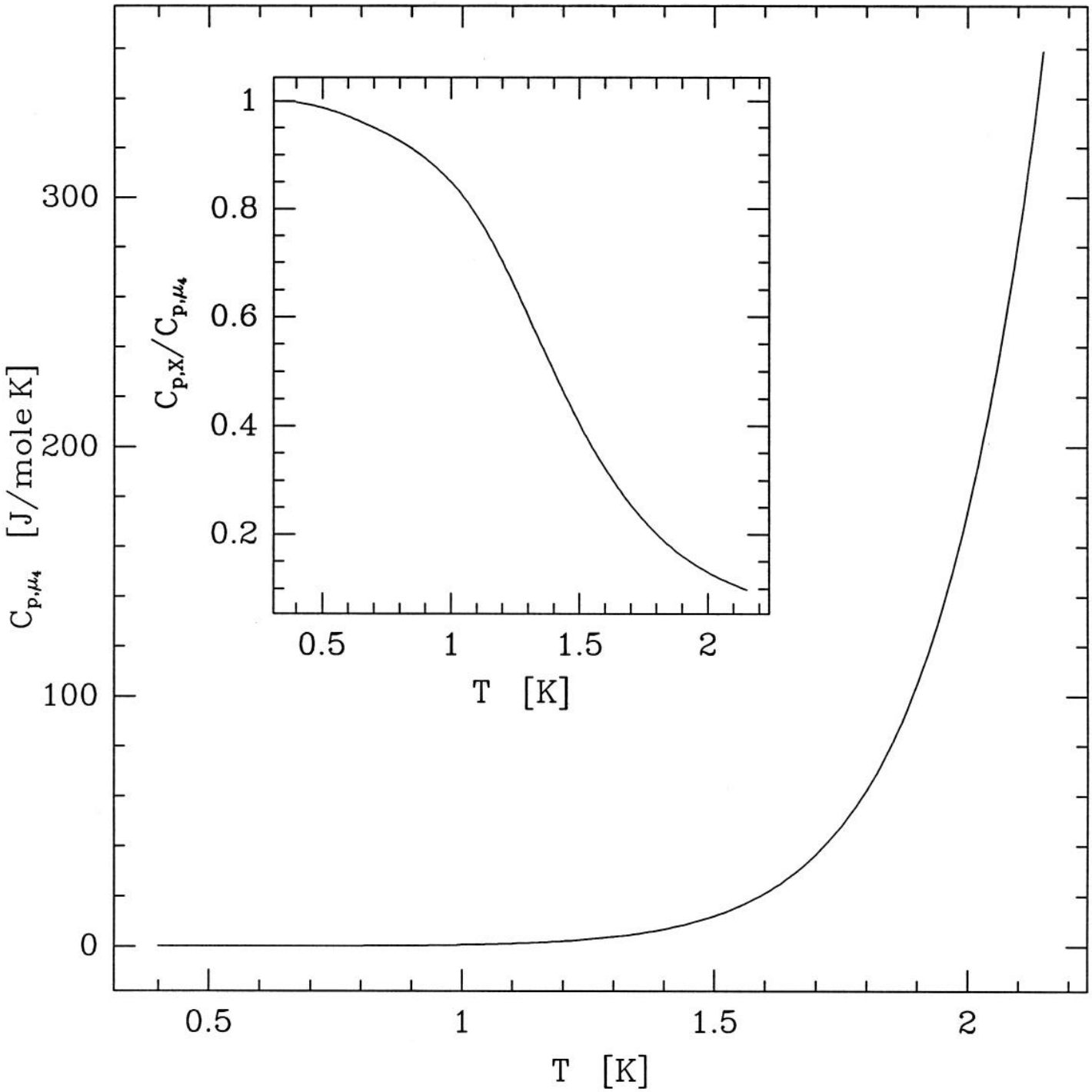
300
200
100
0
C_{p,μ_4} [J/mole K]
0.5
1
1.5
2
T [K]
1
0.8
0.6
0.4
0.2
$C_{p,X}/C_{p,\mu_4}$
0.5
1
1.5
2
T [K]

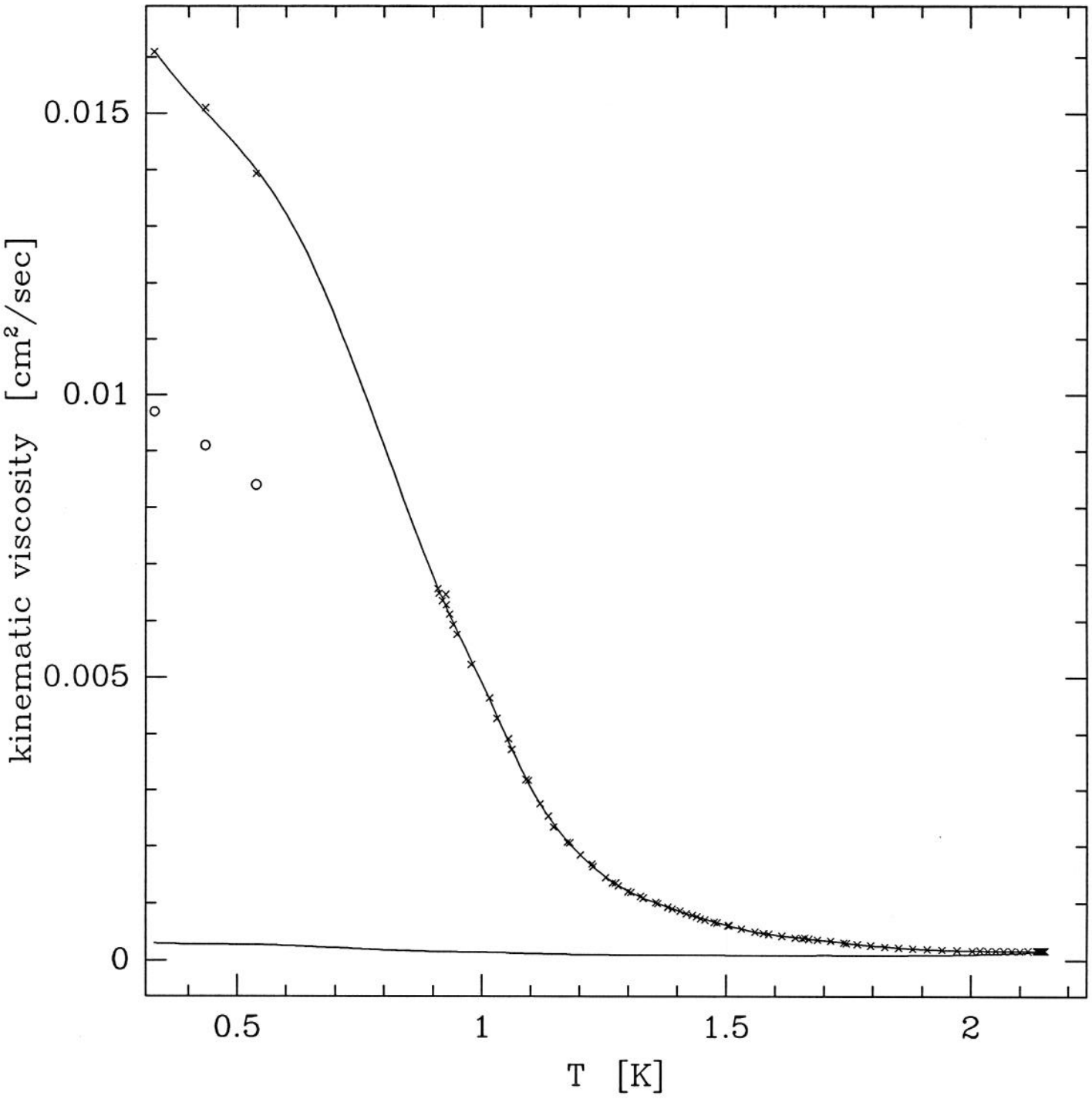
0.015
0.01
0.005
0
kinematic viscosity [cm²/sec]
0.5
1
1.5
2
T [K]

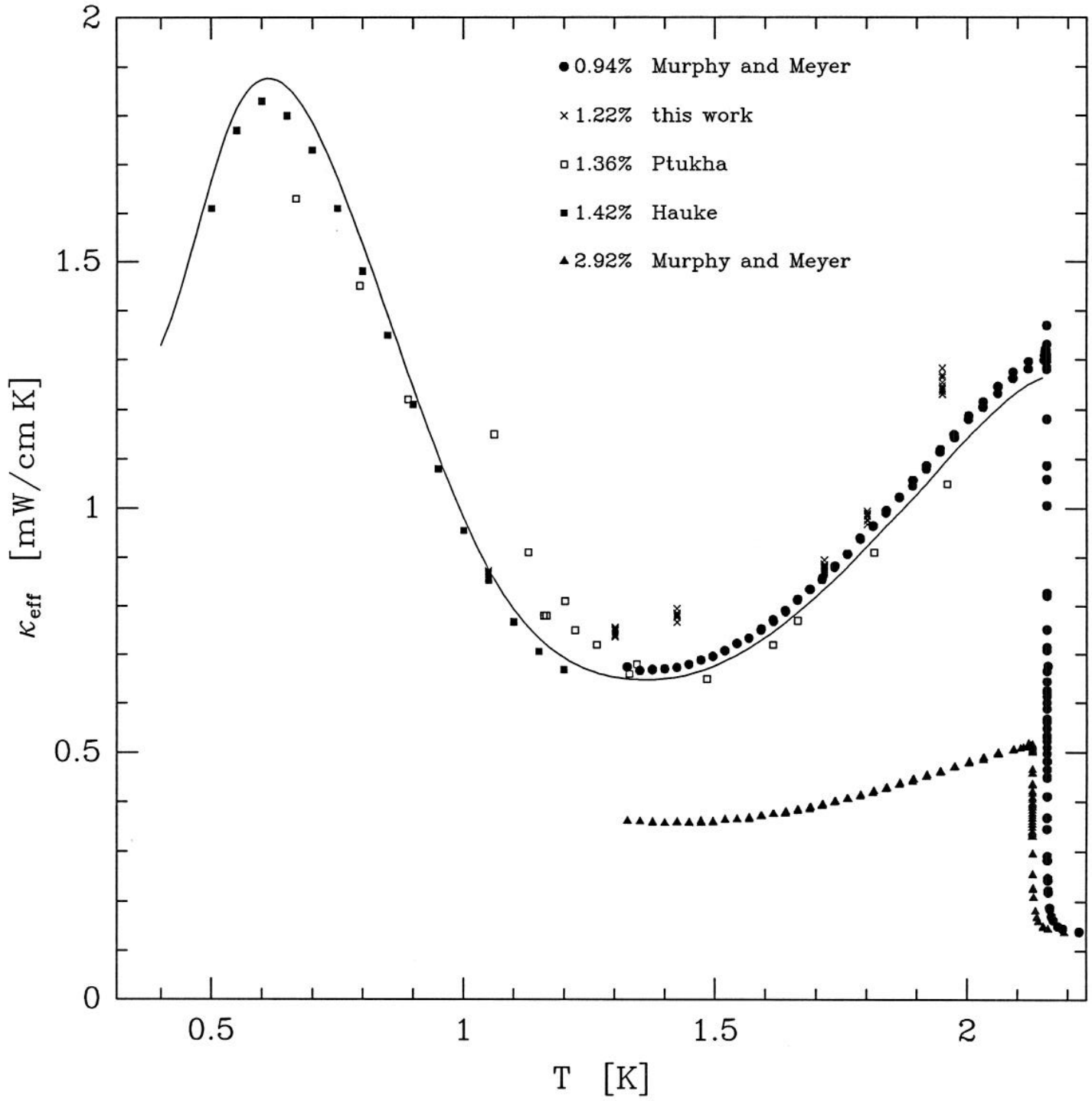
0.94% Murphy and Meyer
1.22% this work
1.36% Ptukha
1.42% Hauke
2.92% Murphy and Meyer
κ_{eff} [mW/cm K]
T [K]
0
0.5
1
1.5
2
0.5
1
1.5
2

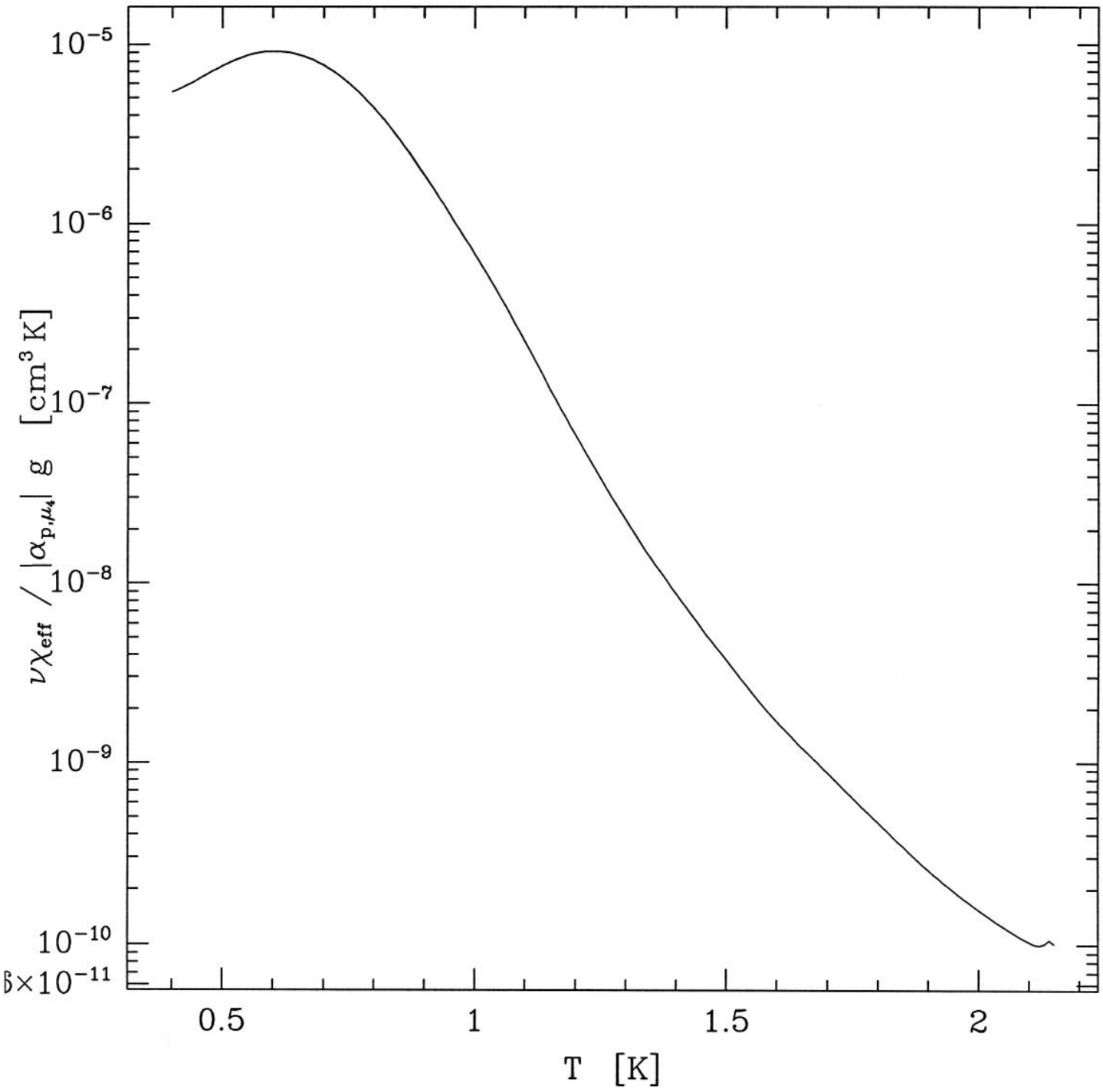
10^{-5}
10^{-6}
10^{-7}
10^{-8}
10^{-9}
10^{-10}
$\times 10^{-11}$
$\nu\chi_{\mathrm{eff}} / |\alpha_{p,\mu_4}|$ g [cm^3 K]
0.5
1
1.5
2
T [K]

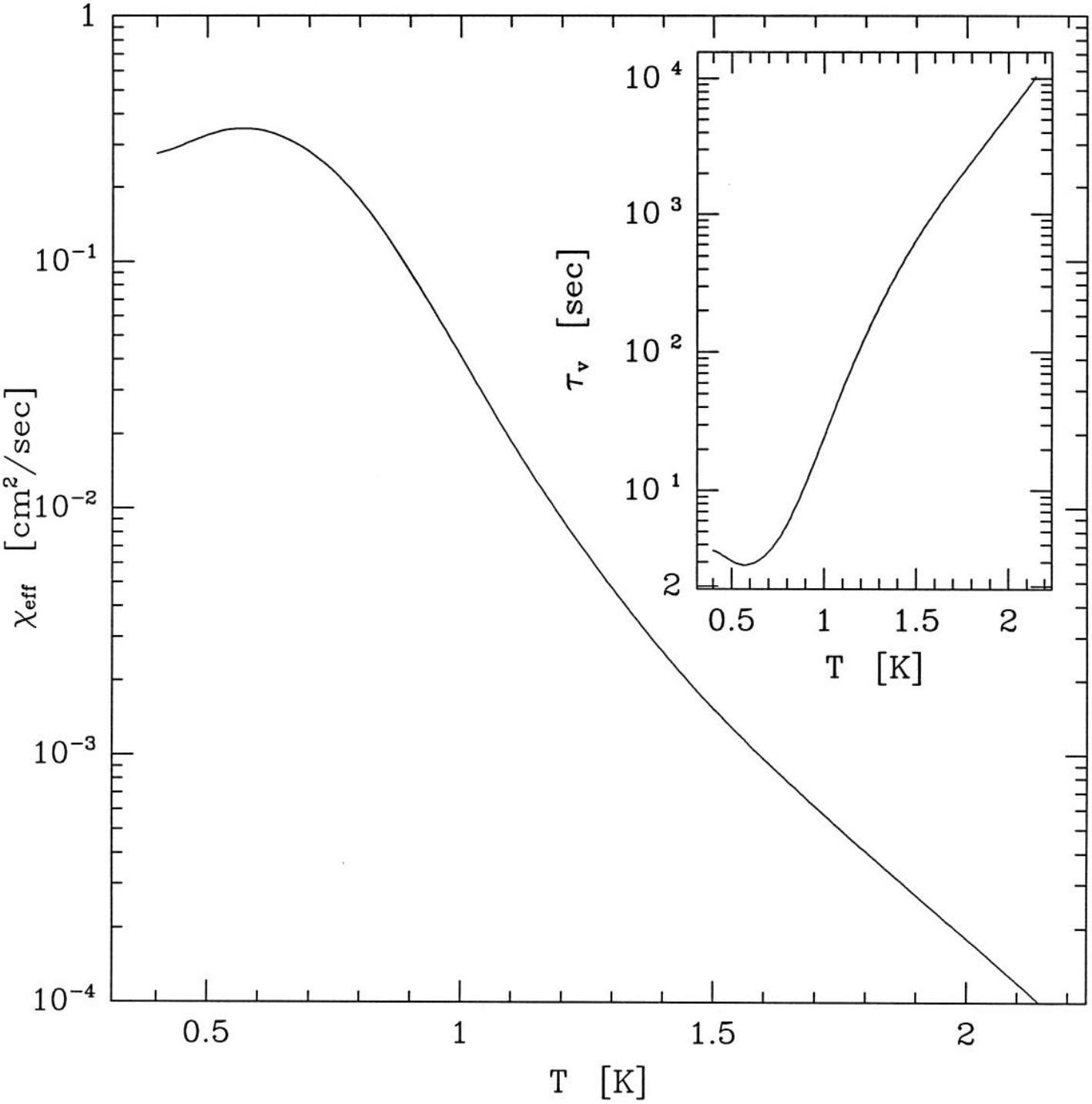
1
10^{-1}
10^{-2}
10^{-3}
10^{-4}
χ_{eff} [cm^2/sec]
0.5
1
1.5
2
T [K]
10^4
10^3
10^2
10^1
2
τ_v [sec]
0.5
1
1.5
2
T [K]